Interplay between Ca- and Ti-driven ferroelectric distortions in (Ba, Ca)TiO 3 solid solutions from first-principles calculations

Danila Amoroso, Andres Cano, Philippe Ghosez

Applied Physics Letters

Interplay between Ca- and Ti-driven ferroelectric distortions in (Ba, Ca)TiO_3 solid solutions from first-principles calculations

Cite as: Appl. Phys. Lett. **114**, 092902 (2019); https://doi.org/10.1063/1.5065655
Submitted: 11 October 2018 . Accepted: 16 February 2019 . Published Online: 04 March 2019

Danila Amoroso, Andrés Cano, and Philippe Ghosez

Applied Physics Letters ARTICLE scitation.org/journal/apl

Interplay between Ca- and Ti-driven ferroelectric distortions in (Ba, Ca)TiO_3 solid solutions from first-principles calculations

Cite as: Appl. Phys. Lett. **114**, 092902 (2019); doi: 10.1063/1.5065655
Submitted: 11 October 2018 · Accepted: 16 February 2019 ·
Published Online: 4 March 2019

Danila Amoroso,[1,2,a),c)] Andrés Cano,[2,b)] and Philippe Ghosez[1]

AFFILIATIONS

[1]Physique Théorique des Matériaux, Q-MAT, CESAM, Université de Liège (B5), B-4000 Liège, Belgium
[2]ICMCB, CNRS, Université de Bordeaux, UMR 5026, F-33600 Pessac, France

[a)]**Present address:** National Research Council CNR-SPIN, c/o Università degli Studi "G. D'Annunzio," I-66100 Chieti, Italy
[b)]**Present address:** Institut Néel, CNRS, UPR 2940, F-38042 Grenoble, France
[c)]**Author to whom correspondence should be addressed:** danila.amoroso@spin.cnr.it.

ABSTRACT

$(Ba,Ca)(Ti,Zr)O_3$ solid solutions are promising lead-free piezoelectrics near their polymorphic phase boundary, which is believed to be linked to the interplay between *B*-site driven ferroelectricity and *A*-site driven ferroelectricity. Focusing on $(Ba,Ca)TiO_3$, we support this picture from first-principles calculations. In particular, we show how steric effects related to the partial substitution of Ba by Ca largely enhance the Ca-driven ferroelectricity, already virtually allowed in the parent $CaTiO_3$. The emergent interplay between the Ca-driven and Ti-driven mechanisms lowers the energy barrier between different polar states, which eventually results in a quasi-isotropic polarization under substitution of a small concentration of Ba by Ca. A sizeable enhancement of the piezoelectric response directly results from these features.

At present, there is a renewed interest in the search of alternative lead-free piezoelectrics. This has led to the identification of very interesting piezoelectric features in $(Ba,Ca)(Ti,Zr)O_3$ (BCTZ) solid solutions.[1] Similar to $Pb(Zr,Ti)O_3$ (PTZ),[2,3] these features are found near a special point in the temperature-composition phase diagram at which the cubic paraelectric phase meets the rhombohedral, orthorhombic, and tetragonal ferroelectric ones.[1,4] This is the so-called polymorphic phase boundary (PPB),[6] which is believed to be promoted by the coexistence of the *B*-site driven ferroelectricity and *A*-site driven ferroelectricity.[7–9] In view of this, the enhanced piezoelectricity in BCTZ is believed to emerge in relation to a rather flat and nearly isotropic energy landscape in which the polarization can easily rotate in all spatial directions.[1,5]

In this letter, we scrutinize this guiding principle by focusing on the dynamical and ferroelectric properties of the parent solid solution $(Ba,Ca)TiO_3$ (BCT). By means of first-principles calculations, we show that the competition between the *B*-type ferroelectricity and *A*-type ferroelectricity promoted by the partial atomic substitution of Ba with Ca results in the reduction and eventually suppression of the energy barrier between the different polar phases, yielding enhanced piezoelectric properties. This confirms that the beneficial overall anisotropy of the system is essentially controlled by the *A*-site substitution of $BaTiO_3$. Moreover, we show that the Ca-driven polar distortion in the solid solution primarily arises from a negative pressure effect exerted by the $BaTiO_3$ matrix on Ca atoms.

We rely on first-principles calculations based on Density Functional Theory (DFT) within the generalized gradient approximation (GGA) using the Wu-Cohen (WC) functional.[10] These calculations are done using the ABINIT package.[11–14] We simulate the solid solutions using 40-atom supercells ($2 \times 2 \times 2$ repetition of 5-atom perovskite unit cell as illustrated in Fig. 1), with $8 \times 8 \times 8$ *k*-mesh and 45 Ha as energy cutoff for the expansion of the electronic wavefunctions, for which energy is converged below ~0.50 meV/f.u. (per 5-atom cell). The structural energy minimization of the supercells has been obtained by fully relaxing lattice vectors and atomic positions starting with different initial conditions related to phases of different symmetries with polarization pointing along different directions. The absolute force tolerance for the structural optimization reached values of about $\sim 10^{-3}$ eV/Å.

Structural distortions of ABO_3 perovskites can be rationalized in terms of the Goldschmidt tolerance factor: $t = (r_O + r_A)/[\sqrt{2}(r_O + r_B)]$, where r_A, r_B, and r_O are the ionic radii of the *A*, *B*, and O ions, respectively.[16]

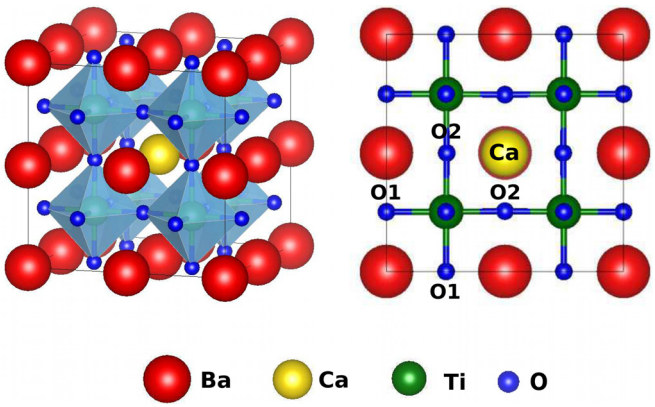

FIG. 1. Schematic representation of the $2 \times 2 \times 2$ supercells for $Ba_{0.875}Ca_{0.125}TiO_3$. In the right panel, oxygen labels help the visualization of the Ti-O atomic pairs in the centro-symmetric structure discussed in the text. Figures have been produced by using the VESTA package.[15]

In $BaTiO_3$ (BTO), $t = 1.06 > 1$ indicates that the Ti ion is too small for its site so that it can easily off-center. As a result, $BaTiO_3$ displays *B*-site driven ferroelectricity with the polar distortion pattern consisting of the opposite motion of Ti cations and O anions [see Fig. 2(g)]. The energies of the three polar phases associated with different directions of polarization are shown in Fig. 2(a), which are in line with the sequence of phase transitions observed experimentally.[19] Specifically, the ground-state corresponds to the rhombohedral phase since maximum energy gain is obtained with polar distortions along the [111] direction.[17–20] Interestingly, the anisotropy of the energy landscape and polarization is linked to the corresponding polar mode[20] and remains qualitatively unaffected by strain relaxation as we show in Figs. 2(a), 2(d), and 3(a), 3(b). This is the signature of a relatively weak polarization-strain coupling in $BaTiO_3$.[17] Accordingly, the calculated *c*/*a* ratio in the tetragonal phase is only ∼1.02. Nevertheless, such coupling remains important for the energy balance between the different polar phases in BCT solid solution, as we will see later.

In $CaTiO_3$ (CTO), on the contrary, $t = 0.97 < 1$ because of the relative small size of Ca. Consequently, the ferroelectric distortion is replaced by tilts and rotations of the TiO_6 octahedra that preserve inversion symmetry. However, $CaTiO_3$ still hosts ferroelectric instabilities in the cubic phase (see Refs. 21–23) and it is known to be an incipient ferroelectric.[24,25] As expected from its *t* value, these ferroelectric instabilities are dominated by the opposite motion of Ca and oxygens, while Ti off-centering is drastically reduced, resulting in *A*-site driven ferroelectricity as illustrated in Fig. 2(i). Unlike in $BaTiO_3$, the tetragonal structure of $CaTiO_3$ is much lower in energy than the orthorhombic and rhombohedral ones. However, we note that the initial instability is relatively isotropic[23] and the strain coupling is now crucial to obtain the eventual anisotropy as we show in Figs. 2(c) and 2(f). Accordingly, the calculated *c*/*a* ratio in the tetragonal phase becomes ∼1.06. The amplification of Ca-displacements obtained by taking the polarization-strain coupling into account is another manifestation of the importance of such coupling in $CaTiO_3$, as shown in Figs. 3(d) and 3(e).

Such large strain coupling was previously reported in compounds with a stereochemically active lone pair at the *A*-site like $PbTiO_3$[26,31] and $BiFeO_3$.[27,28] However, the above fact indicates that it is a more generic feature of *A*-type ferroelectrics. In fact, a similar behavior also affects $CaZrO_3$,[23,29] with a calculated $c/a \simeq 1.07$ in the *P*4*mm* structure.

In view of the above fact, it can be anticipated that the partial substitution of Ba by Ca in $BaTiO_3$ can promote the coexistence of competing Ti-driven ferroelectricity and Ca-driven ferroelectricity and thus affect the polarization anisotropy. Calculations on $Ba_{1-x}Ca_xTiO_3$ confirm this expectation. The three distinct ferroelectric states of $BaTiO_3$ ($x = 0$) become quasi-degenerate in energy for $x = 0.125$, as illustrated in Fig. 2(b). On average, the energy lowering with respect to the paraelectric cubic structure is about ∼−20 meV/f.u. in both cases. However, the energy dispersion between the different polar phases is reduced from 5 meV/f.u. for $x = 0$ to below 0.5 meV/f.u. for $x = 0.125$.[23] In particular, the energy of the tetragonal phase is lower than in $BaTiO_3$. This is because of the large *A*-site character of the polar distortion brought by the Ca substitution. Interestingly, this quasi-degeneracy can be reproduced via a simple heuristic model in which the relative energy of each ferroelectric phase (E^i) and its spontaneous polarization (P^i) are expressed as a linear combination of the corresponding quantities of the parent compounds

$$E^i(x) = (1-x)E^i_{BTO} + xE^i_{CTO}, \quad (1)$$

$$P^i(x) = (1-x)P^i_{BTO} + xP^i_{CTO}, \quad (2)$$

where *x* is the Ca concentration. This simple model exploits the reversed sequence of ferroelectric states displayed by the two parent compounds. Noteworthy, the strain effect has to be included to properly reproduce the quasi-degeneracy of phases. The obtained from this model is shown in Figs. 2(b) and 2(e).

Going back to the specific results from supercell calculations for $x = 0.125$, it is noteworthy that the quasi-degeneracy in energy of the tetragonal, orthorhombic, and rhombohedral phases allows the emergence of other competing polarization states. In particular, we find a new metastable triclinic-$P1(C_1)$ phase with polarization P_{abc} nearly between the [001]-[111] directions of the original cubic structure ($P_a/P_c \simeq 0.53$, $P_b/P_c \simeq 0.48$) and a monoclinic-$Pm(C_1^s)$ phase with polarization P_{0bc} in between the [001]-[011] directions ($P_b/P_c \simeq 0.53$) [Figs. 2(b) and 2(e)]. Furthermore, the spontaneous polarization and related atomic distortions are essentially the same for all the ferroelectric phases as we show in Figs. 2(e) and 2(h) [$P \sim 39\ \mu C/cm^2$ (Ref. 23) as computed via the Berry phase[30]]. Together with the quasi-degeneracy of the energies, these results disclose a remarkably isotropic energy landscape.

As a result, the piezoelectric response for this composition is significantly enhanced compared to the parent $BaTiO_3$. Specifically, if we consider the rhombohedral phase, there is a substantial enhancement of the transversal components that become up to 5 times larger. Values were already published in Ref. 23.

We note also in Fig. 2(h) that, in the solid solution at $x = 0.125$, both the displacements of Ti and O atoms and the relative (Ti-O) motion remain almost the same as in the parent $BaTiO_3$ phase, while the displacement of Ca is much larger than that of Ba, thus enhancing the average *A*-site contribution to the polar distortion, in agreement with experimental observations reported in Refs. 29, 34, and 35. As it will be further discussed later, the Ca motion is related to local steric effects and appears to be even larger in the solid solution than in the parent $CaTiO_3$ phase. Nevertheless, the average displacement of O atoms is now reduced if compared to $CaTiO_3$ due to the fact that O

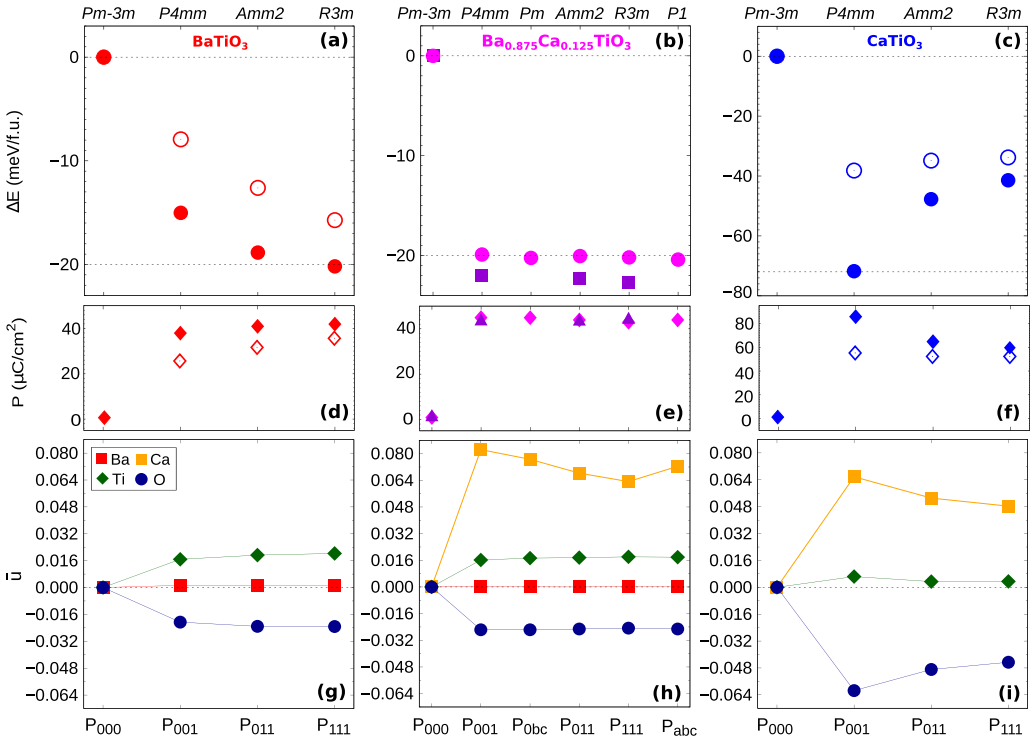

FIG. 2. Comparison of the energetics, spontaneous polarization, and atomic displacements for (a), (d), and (g) $BaTiO_3$, (b), (e), and (h) $Ba_{0.875}Ca_{0.125}TiO_3$, and (c), (f), and (i) $CaTiO_3$. (Top) Energy gain (in meV/f.u.) relative to the cubic reference for states with different orientations of polarization. Closed circles represent structures relaxed both in the atomic positions and volume. In (a) and (c), open circles reproduce the energy-lowering associated with the polar distortion within the fixed cubic unit cell (i.e., no strain relaxation) for $BaTiO_3$ and $CaTiO_3$, respectively. For $Ba_{0.875}Ca_{0.125}TiO_3$, (b) closed squares reproduce the energetics as obtained from Eq. (1). (Center) Trend of spontaneous polarization (in $\mu C/cm^2$) calculated by means of computed atomic displacements and Born effective charges, $P_{s,\alpha} = \frac{1}{\Omega}\sum_{k,\beta} Z^*_{k,\alpha\beta}\Delta\tau_{k,\beta}$,[32] for different polar states. In (d) and (f), open rhombi reproduce polarization constrained to the cubic unit cell for $BaTiO_3$ and $CaTiO_3$, respectively. For $Ba_{0.875}Ca_{0.125}TiO_3$, (e) closed triangles reproduce the polarization as obtained from Eq. (2). (Bottom) Evolution of average atomic displacements (in internal coordinates) relative to the center of mass of corresponding cells. Values are scaled to the 5-atom cell to allow comparison. The reported sign for $\bar{u}$ helps the visualization of the opposite cation-anion motion.

atoms belong to the overall BTO-matrix. Therefore, the relative Ca-O motion remains comparable to the one in $CaTiO_3$, thus making the Ca-O total contribution to the spontaneous polarization almost similar to that in $CaTiO_3$. This explains qualitatively why the spontaneous polarization interpolates linearly with x according to Eq. (2). Furthermore, the Ca-Ca interatomic interaction in $CaTiO_3$ has been shown to be rather weak,[23] so that Ca displacement does not require long-range cooperative motions in real space, thus making this

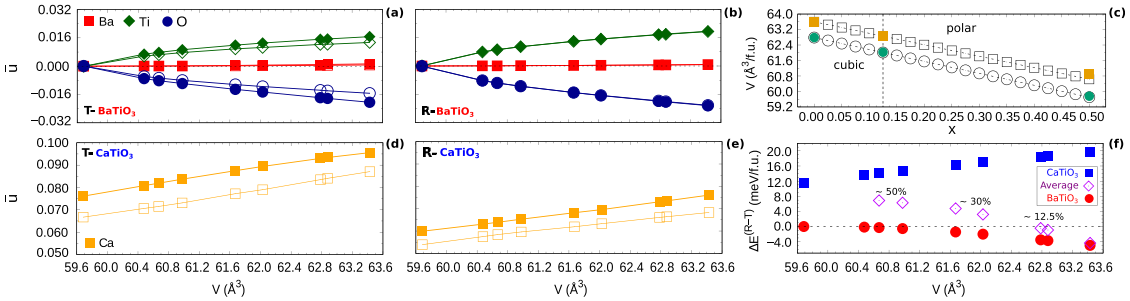

FIG. 3. Atomic displacements (in internal coordinates) and energetics as a function of the volume of the unit cell. (a) and (b) Ba, Ti, and O displacements in *T*-tetragonal and *R*-rhombohedral $BaTiO_3$. (d) and (e) Ca displacement in *T*- and *R*-$CaTiO_3$. Closed (open) symbols refer to constant-volume optimization with (without) internal strain relaxation. (c) Averaged volume as a function of the composition *x* for the cubic and polar phases. Closed symbols represent the calculated volumes, while open symbols are extrapolated according to Vegard's law. (f) Relative energy difference between the *R* and *T* phases in $BaTiO_3$ and $CaTiO_3$ as a function of the volume ($\Delta E^{R-T} = E_R - E_T$). The internal strain relaxation is considered for $BaTiO_3$ but not for $CaTiO_3$ (so that only the effect of the isotropic tensile expansion is considered in the latter case). Open rhombi correspond to the average $(1-x)\Delta E_{BTO} + x\Delta E_{CTO}$ according to Vegard's law in (c), with the equivalent %-composition indicated in the figure.

mechanism already operative at small Ca concentrations and independent of order/disorder effects.

The specific dynamics in $Ba_{0.875}Ca_{0.125}TiO_3$ is thus a clear manifestation of the interplay between the *B*-site and *A*-site driven characters of the polar distortion.

As we show in the following, these features can be understood microscopically due to steric effects related to the different sizes of barium and calcium cations.

The ionic radii of Ba and Ca are 1.61 Å and 1.34 Å, respectively,[16] and the calculated volume of $BaTiO_3$ in the high-reference cubic phase is more than 10% larger than that of $CaTiO_3$, i.e., 62.784 $Å^3$ for $BaTiO_3$ and 56.623 $Å^3$ for $CaTiO_3$. In agreement with experimental data reported by Levin *et al.* in Ref. 34, we find that the volume of BCT monotonically decreases with the Ca-concentration following Vegard's law [Fig. 3(c)]. In particular, the calculated volume of cubic $Ba_{0.875}Ca_{0.125}TiO_3$ is 62.028 $Å^3$/f.u. From one hand, this corresponds to an overall ∼1.2% contraction of the $BaTiO_3$ volume, although the local strain effect on the Ti-O distances is anisotropic being alternately tensile and compressive, i.e., $Ti\text{-}O_1 \simeq 1.994$ Å and $Ti\text{-}O_2 \simeq 1.965$ Å, where labels refer to Fig. 1. On the other hand, it corresponds to a virtually ∼9.5% expansion of the $CaTiO_3$ volume. In particular, to accommodate the difference in size introduced by the substitution of one Ba with one Ca, a structural relaxation takes place around the single Ca-impurity, corresponding now to isotropic tensile stress being Ca-Ba distances ≃3.9585 Å and Ca-O distances ≃2.7504 Å in all directions. This, in turn, strongly affects the contribution of Ca-motion to the polar distortion and to the energy balance between the polar phases in the solid solution.

Accordingly, we studied the evolution of the displacements of Ti and O atoms in $BaTiO_3$ and of Ca in $CaTiO_3$ as a function of volume and of the difference of energy between tetragonal and rhombohedral polar phases. In detail, we fixed the volume to the expected average volumes associated with polar phases at different Ca-concentrations, following Vegard's law (Fig. 3). Then, in order to disentangle the effect of the external isotropic stress induced by the atomic substitution from that of the polarization-strain coupling internal to each system, we performed atomic relaxation at constant volume and cubic cell geometry for the first case (i.e., no internal strain relaxation), with additional unit cell shape relaxation for the second case (i.e., with internal strain relaxation).

The Ti-O polar motion smoothly tends to zero as a function of contracted volumes in $BaTiO_3$, as shown in Figs. 3(a) and 3(b). This corresponds in fact to the known suppression of ferroelectricity in $BaTiO_3$ by compressive stress via modification of the Ti-O interatomic interactions.[23,33] Nevertheless, at the volume size corresponding to the one from $x = 0.125$, the relative Ti-O displacements are still very close to those in pure $BaTiO_3$ and reproduce the displacements as obtained in the supercell [compare Figs. 3(a) and 3(b) to Fig. 2(h)].

Differently, the polar motion of Ca is strongly enhanced due to volume expansion when compared to the unstrained parent $CaTiO_3$ [compare Figs. 3(d) and 3(e) to Fig. 2(i)]. In fact, the Ca-O interatomic interaction, which sustains the *A*-site driven polar distortion in $CaTiO_3$,[23] turns out to be strengthened by increasing volume (not shown here). Moreover, the displacement of Ca as obtained in the supercell for $x = 0.125$ is well reproduced by simulating $CaTiO_3$ under isotropic tensile stress. The inclusion of the internal polarization-strain coupling remarkably increases the Ca-motion, confirming a strong polarization-strain coupling in $CaTiO_3$.

This study thus reveals how the volume expansion strongly enhances the polar motion of Ca at the *A*-site, thus making the Ca-driven polar distortion competing with the Ti-driven one in BCT and in BCTZ solid solutions.

We can now consider the effect of these features on the energetics associated with the tetragonal and rhombohedral phases. The trend of the relative energy gain between the two polar phases in Fig. 3(f) and its comparison with the energetics in Figs. 2(a) and 2(c) point out that volume contraction smoothly reduces the energy difference between the tetragonal and rhombohedral phases in $BaTiO_3$, while volume expansion largely favors the tetragonal phase over the rhombohedral one in $CaTiO_3$. Then, by combining linearly the relative energy gain of $BaTiO_3$ and of $CaTiO_3$, we see that this difference in energy goes nearly to zero for $x \simeq 0.125$, thus reproducing the quasi-degeneracy of polar phases obtained in $Ba_{0.875}Ca_{0.125}TiO_3$ by means of supercell calculations, as shown in Fig. 3(f). In particular, this is true if we take into account the contribution of both external induced volume effects and internal polarization-strain relaxation for $BaTiO_3$ and the contribution of external isotropic volume expansion alone for $CaTiO_3$. This means that our specific calculations for $x \simeq 0.125$ performed on $2 \times 2 \times 2$ supercells are well reproduced, modeling the system as a BTO-matrix which exerts a negative hydrostatic pressure on Ca. More generally, the usual polarization-strain coupling of $CaTiO_3$ is not playing any significant role at small Ca-substitution concentrations. Then, the agreement for $x \simeq 0.50$ is only qualitative if we compare the obtained energetics with the one reported for $Ba_{0.50}Ca_{0.50}TiO_3$ solid solutions in Ref. 23 [Fig. 8(c)]. This is due to the fact that the higher the calcium concentration, the more all the strain-relaxation effects are interconnected and not negligible.

This simple study reveals how volume expansion has a strong effect on the $CaTiO_3$ energetics and is responsible for the stabilization of the tetragonal phase in the BCT phase diagram already for $x \gtrsim 0.23$.[9,36] In addition to the latter, all our calculations also reveal that the inversion of the energy sequence of ferroelectric states, which characterizes the end members $BaTiO_3$ and $CaTiO_3$, occurs in BCT through a quasi-degeneracy in energy of the polar phases for small Ca-concentration *x*. This, in turn, produces a minimal anisotropy condition with respect to different polarization states, eventually allowing for the enhancement of the piezoelectric response.

Despite being based on specific ordered systems, our whole analysis thus provides a reliable microscopic understanding of the mechanisms behind the interplay between the Ti-driven ferroelectricity and Ca-driven ferroelectricity and the related effect on the overall anisotropy in BCT. This also provides then an insight into some of the mechanisms playing a role in Ba-rich BCTZ solid solutions.

In summary, we have performed a first-principles study of $(Ba,Ca)TiO_3$ that sheds light on the relationships between coexistent (Ti,Ca)-driven ferroelectricity and energy competition between different polar phases, at the basis of the polymorphic phase boundary of the $(Ba,Ca)(Ti,Zr)O_3$ solid solutions. Our study reveals that the competing interplay between the two mechanisms driving ferroelectricity is promoted by steric effects: the volume expansion experienced by Ca inside the solid solution largely enhances the Ca-driven contribution to the polar distortion, favoring the tetragonal phase and destabilizing the rhombohedral one. An energy competition between various polarization states thus occurs for small substitution concentrations of Ca, yielding a quasi-isotropic energy landscape. Therefore, solid solutions

with possible mixing of *B*-type ferroelectricity and *A*-type ferroelectricity seem to be a promising guideline in designing high-performing lead-free piezoelectrics.

D.A. is grateful to S. Picozzi (CNR-SPIN) for the provided time needed for writing this paper and to B. Dkhil (Centrale-Supléc) for enlightening discussions. Ph.G. acknowledges the support of the F.R.S-FNRS Hit4Fit project. This work was supported by the European project EJD-FunMat 2015 and program H2020-MSCA-ITN-2014 under Grant Agreement No. 641640. Calculations have been performed on the Céci facilities funded by F.R.S-FNRS (Grant No. 2.5020.1) and on the Tier-1 supercomputer of the Fédération Wallonie-Bruxelles funded by the Walloon Region (Grant No. 1117545).

REFERENCES

[1]W. Liu and X. Ren, Phys. Rev. Lett. **103**, 257602 (2009).
[2]R. Guo, L. E. Cross, S.-E. Park, B. Noheda, D. E. Cox, and G. Shirane, Phys. Rev. Lett. **84**, 5423 (2000).
[3]B. Noheda, J. A. Gonzalo, L. E. Cross, R. Guo, S.-E. Park, D. E. Cox, and G. Shirane, Appl. Phys. Lett. **74**, 2059 (1999).
[4]D. S. Keeble, F. Benabdallah, P. A. Thomas, M. Maglione, and J. Kreisel, Appl. Phys. Lett. **102**, 092903 (2013).
[5]H. Fu and R. E. Cohen, Nature **403**, 281 (2000).
[6]M. Acosta, N. Novak, V. Rojas, S. Patel, R. Vaish, J. Koruza, G. A. Rossetti, and J. Rödel, Appl. Phys. Rev. **4**, 041305 (2017).
[7]M. Ghita, M. Fornari, D. J. Singh, and S. V. Halilov, Phys. Rev. B **72**, 054114 (2005).
[8]D. I. Bilc and D. J. Singh, Phys. Rev. Lett. **96**, 147602 (2006).
[9]D. Fu, M. Itoh, S. Ya Koshihara, T. Kosugi, and S. Tsuneyuki, Phys. Rev. Lett. **100**, 227601 (2008).
[10]Z. Wu and R. E. Cohen, Phys. Rev. B **73**, 235116 (2006).
[11]X. Gonze, J.-M. Beuken, R. Caracas, F. Detraux, M. Fuchs, G.-M. Rignanese, L. Sindic, M. Verstraete, G. Zerah, F. Jollet, M. Torrent, A. Roy, M. Mikami, P. Ghosez, J.-Y. Raty, and D. C. Allan, Comput. Mater. Sci. **25**, 478 (2002).
[12]X. Gonze, G.-M. Rignanese, M. Verstraete, J.-M. Beuken, Y. Pouillon, R. Caracas, F. Jollet, M. Torrent, G. Zerah, M. Mikami, P. Ghosez, M. Veithen, J.-Y. Raty, V. Olevano, F. Bruneval, L. Reining, R. Godby, G. Onida, D. R. Hamann, and D. C. Allan, Z. Kristallogr. **220**, 558 (2005).
[13]X. Gonze, B. Amadon, P.-M. Anglade, J.-M. Beuken, F. Bottin, P. Boulanger, F. Bruneval, D. Caliste, R. Caracas, M. Cote, T. Deutsch, L. Genovese, P. Ghosez, M. Giantomassi, S. Goedecker, D. R. Hamann, P. Hermet, F. Jollet, G. Jomard, S. Leroux, M. Mancini, S. Mazevet, M. J. T. Oliveira, G. Onida, Y. Pouillon, T. Rangel, G.-M. Rignanese, D. Sangalli, R. Shaltaf, M. Torrent, M. J. Verstraete, G. Zerah, and J. W. Zwanziger, Comput. Phys. Commun. **180**, 2582 (2009).
[14]See www.abinit.org for ABINIT technicalities.
[15]K. Momma and F. Izumi, J. Appl. Crystallogr. **44**, 1272 (2011).
[16]R. D. Shannon, Acta Cryst. A **32**, 751 (1976).
[17]R. E. Cohen and H. Krakauer, Phys. Rev. B **42**, 6416 (1990).
[18]A. F. Devonshire, Philos. Mag. **40**, 1040 (1949); **42**, 1065 (1951); Adv. Phys. **3**, 85 (1954).
[19]G. H. Kwei, A. C. Lawson, S. J. L. Billinge, and S.-W. Cbeong, J. Phys. Chem. **97**, 2368 (1993).
[20]P. Ghosez, X. Gonze, and J.-P. Michenaud, Ferroelectrics **206**, 205 (1998).
[21]K. Parlinski, Y. Kawazoe, and Y. Waseda, J. Chem. Phys. **114**, 2395 (2001).
[22]S. Amisi, E. Bousquet, K. Katcho, and P. Ghosez, Phys. Rev. B **85**, 064112 (2012).
[23]D. Amoroso, A. Cano, and P. Ghosez, Phys. Rev. B **97**, 174108 (2018).
[24]V. V. Lemanov, A. V. Sotnikov, E. P. Smirnova, M. Weihnacht, and R. Kunze, Solid State Commun. **110**, 611 (1999).
[25]Y. Gu, K. Rabe, E. Bousquet, V. Gopalan, and L.-Q. Chen, Phys. Rev. B **85**, 064117 (2012).
[26]K. M. Rabe and U. V. Waghmare, Philos. Trans. R. Soc. London A **354**, 2897 (1996).
[27]C. Ederer and N. A. Spaldin, Phys. Rev. Lett. **95**, 257601 (2005).
[28]A. J. Hatt, N. A. Spaldin, and C. Ederer, Phys. Rev. B **81**, 054109 (2010).
[29]J. W. Bennett, I. Grinberg, and A. M. Rappe, Chem. Mater. **20**, 5134 (2008).
[30]R. D. Smith and D. Vanderbilt, Phys. Rev. B **47**, 1651 (1993).
[31]R. E. Cohen, J. Phys. Chem. Solids **61**, 139 (2000).
[32]P. Ghosez, J.-P. Michenaud, and X. Gonze, Phys. Rev. B **58**, 6224 (1998).
[33]E. Bousquet and P. Ghosez, Phys. Rev. B **74**, 180101 (2006).
[34]I. Levin, V. Krayzman, and J. C. Woicik, Appl. Phys. Lett. **102**, 162906 (2013).
[35]I. B. Ouni, D. Chapron, H. Aroui, and M. D. Fontana, J. Appl. Phys. **121**, 114102 (2017).
[36]T. Mitsui and W. B. Westphal, Phys. Rev. **124**, 1354 (1961).